HHS Public Access

Author manuscript

J Mol Med (Berl). Author manuscript; available in PMC 2025 January 08.

Published in final edited form as:

J Mol Med (Berl). 2013 May ; 91(5): 561–572. doi:10.1007/s00109-012-0973-1.

The chloride channel/transporter Slc26a9 regulates the systemic arterial pressure and renal chloride excretion

Hassane Amlal,
Research Services, Veterans Affairs Medical Center, Cincinnati, OH, USA; Department of Medicine, University of Cincinnati, Cincinnati, OH, USA; Center on Genetics of Transport and Epithelial Biology, University of Cincinnati, Cincinnati, OH, USA

Jie Xu,
Research Services, Veterans Affairs Medical Center, Cincinnati, OH, USA; Department of Medicine, University of Cincinnati, Cincinnati, OH, USA; Center on Genetics of Transport and Epithelial Biology, University of Cincinnati, Cincinnati, OH, USA

Sharon Barone,
Research Services, Veterans Affairs Medical Center, Cincinnati, OH, USA; Department of Medicine, University of Cincinnati, Cincinnati, OH, USA; Center on Genetics of Transport and Epithelial Biology, University of Cincinnati, Cincinnati, OH, USA

Kamyar Zahedi,
Research Services, Veterans Affairs Medical Center, Cincinnati, OH, USA; Department of Medicine, University of Cincinnati, Cincinnati, OH, USA; Center on Genetics of Transport and Epithelial Biology, University of Cincinnati, Cincinnati, OH, USA

Manoocher Soleimani
Research Services, Veterans Affairs Medical Center, Cincinnati, OH, USA; Department of Medicine, University of Cincinnati, Cincinnati, OH, USA; Center on Genetics of Transport and Epithelial Biology, University of Cincinnati, Cincinnati, OH, USA; University of Cincinnati, 231 Albert Sabin Way, MSB 6213, Cincinnati, OH 45267-0585, USA

Abstract

Apical chloride secretory pathways in the kidney medullary collecting duct are thought to play an important role in the modulation of final urine composition and regulation of systemic vascular volume and/or blood pressure. However, the molecular identity of these molecules has largely remained unknown. Here, we demonstrate that Slc26a9, an electrogenic chloride channel/transporter, is localized on the apical membrane of principal cells in the kidney medullary collecting duct and mediates chloride secretion. Mice with the genetic deletion of Slc26a9 show significant reduction in renal chloride excretion when fed a diet high in salt or subjected to water deprivation. Arterial pressure measurements indicated that Slc26a9 knockout ($Slc26a9^{-/-}$) mice are hypertensive under baseline conditions and increase their blood pressure further within 48 h of switching to a high-salt diet. These results suggest that Slc26a9 plays an important role in

✉ manoocher.soleimani@uc.edu .

Conflict of interest The authors report no conflict of interest.

renal chloride/fluid excretion and arterial pressure regulation. We propose that impaired SLC26A9 activity in humans may interfere with the excretion of excess salt and result in hypertension.

Keywords

SLC26 isoforms; Hypertension; Kidney medullary collecting duct; Renal chloride excretion; High salt intake

Introduction

The kidney collecting duct plays a major role in vascular volume homeostasis by regulating the reabsorption of sodium, chloride, and fluid [1–5]. The apical sodium channel and AQP2, located on the apical membrane of principal cells, reabsorb sodium and water, respectively [5–7], and the Cl^-/HCO_3^- exchanger SLC26A4 (pendrin), located on the apical membrane of B and non-A, non-B intercalated cells, reabsorbs chloride [8–11]. Several functional studies have identified apical chloride secretory channels in cultured collecting duct cells where they are thought to play an important role in regulating the excretion of chloride and composition of the final urine [12–14]. However, the identity and/or the possible role of such a channel or channels remain speculative.

Solute-linked carrier 26 (SLC26) isoforms belong to a conserved family of anion transporters, many of which display restricted tissue expression and distinct subcellular localization in epithelial tissues, with some isoforms detected exclusively on the apical membrane, whereas others are found on the basolateral membrane or in endosomes [15–20]. SLC26 isoforms can transport various anions, including chloride, sulfate, bicarbonate, and oxalate, with variable specificity. Several SLC26A members function as chloride/bicarbonate exchangers. These include SLC26A3 (DRA), SLC26A4 (pendrin), SLC26A6 (PAT1), SLC26A7, and SLC26A9 [8, 21–26]. SLC26A7 and SLC26A9 can also function as chloride channels [26–29].

SLC26A9 (human)/Slc26a9 (mouse) is abundantly expressed in the stomach and lung, with lower levels in the kidney [25, 29]. It can function in three distinct modes, including electrogenic Cl^-/HCO_3^- exchange, chloride channel, and sodium chloride cotransport [25–29]. In the stomach, Slc26a9 is located on the apical membrane of surface epithelial cells and in tubulovesicles of gastric parietal cells and regulates gastric acid secretion [25, 26]. The nephron segment distribution, subcellular localization, and physiologic role of Slc26a9 in the kidney remain unknown. Our studies demonstrate that Slc26a9 is expressed in the collecting duct and plays a key role in chloride excretion and blood pressure regulation.

Materials and methods

Animal models

Details of Slc26a9 null mice generation were recently reported by our group [26]. $Slc26a9^{+/+}$ and $Slc26a9^{-/-}$ were housed and cared for in accordance with the Institutional Animal Care and Use Committee (IACUC) at the University of Cincinnati. All animal handlers were IACUC-trained. Animals had access to food and water ad libitum, were

housed in humidity-, temperature-, and light/dark-controlled rooms, and were inspected daily. Animals were euthanized with the use of excess anesthetics (pentobarbital sodium) according to institutional guidelines and approved protocols.

Experimental models

The following two models were employed for the current studies:

Water deprivation.—Slc26a9$^{-/-}$ mice and their wild-type (WT) littermates were placed in metabolic cages and fed rodent chow with free access to distilled water. After 3 days of acclimation to metabolic cages, animals were subjected to water deprivation by having their water bottles removed for 24 h. Animals had free access to food during water deprivation. Urine volume, electrolyte excretion, food intake, and body weights were measured daily. After water deprivation, animals were euthanized and tissues and bloods were collected.

Salt loading.—Slc26a9$^{-/-}$ mice and their WT littermates were fed normal-salt (1 %) liquid diet for several days before they were moved to metabolic cages. After 3 days of acclimation to metabolic cages, mice were switched to a high-salt (7 %) liquid diet. Food intake, urine volume, and chloride excretion were monitored daily before and after switching to high-salt diet.

Antibodies

Slc26a9 and Slc26a4 (pendrin) antibodies were generated in our laboratory as described [11, 25, 26]. The antibodies against Slc26a11 (kidney brain anion transporter [KBAT]) were recently generated in our laboratory [30]. The monoclonal AQP2 antibodies [24] were gifts from Dr. Ann Blanchard, Paris, France. The monoclonal antibodies against the 31-kDa subunit of H^+-ATPase were gifts from Dr. Holliday [30].

Blood composition and urine electrolytes analysis

Urine was collected under mineral oil. Serum and urine chloride concentration were measured using a digital chloridometer (HBI Haake Buchler Instruments, Inc., Saddle Brook NJ, USA). Serum concentrations of Na^+, K^+, Ca^{++}, and HCO_3^- were measured in the blood using the i-STAT^R-1 analyzer with i-STAT EG7+ cartridges (Abbott Laboratories, Abbott Park, IL, USA). Urine sodium concentration was measured by flame photometry.

RT-PCR of Slc26a9

Total RNA was prepared from mouse kidney (cortex and medulla) and the cultured cortical and medullary collecting duct cells. It was then reverse transcribed at 42 °C using SuperScript II RT (Life Technologies, Carlsbad, CA, USA) and appropriate oligo(dT) primers. Oligonucleotide primers 5′-GGA ACT CAA CGC TCG GTA CAT G-3′ (sense) and 5′-AAG CTC ACC ACC CAG ACA CAA C-3′ (antisense) were designed based on mouse Slc26a9 sequence (GenBank accession no. NM_177243). The polymerase chain reaction (PCR) conditions were as follows: segment 1, 2 min at 94 °C (denature) 1 cycle; segment 2, 35 cycles of 30 s at 94 °C (denature), 30 s at 65 °C (annealing), 2 min at 68 °C (extension); segment 3, link to 68 °C for 5 min (1 cycle). For control in loading and amplification and quantitation of mRNA levels, GAPDH mRNA was amplified.

Immunofluorescence labeling studies

Animals were euthanized with an overdose of pentobarbital sodium and perfused through the left ventricle with 0.9 % saline followed by cold 4 % paraformaldehyde in 0.1 M sodium phosphate buffer (pH 7.4). Kidneys were removed, cut in tissue blocks, and fixed in formaldehyde solution overnight at 4 °C. The tissue was frozen on dry ice, 6-μm sections were cut with a cryostat, and stored at −80 °C until used. Single immunofluorescence labeling was performed as described [11, 23, 25] using either Alexa Fluor 488 (green) or Alexa Fluor 594 (red) antibody as secondary antibodies.

For double immunofluorescence labeling, polyclonal Slc26a9 antibodies (at 1:30 dilution) were used in conjunction with monoclonal AQP2 (at 1:3,000 dilution). Slc26a11 (KBAT) antibodies were labeled by Alexa Fluor 594 goat antirabbit IgG labeling kit and AQP-2 antibodies were labeled using Alexa Fluor 488 goat antimouse IgG labeling kit (Invitrogen Molecular Probes, Eugene, OR, USA) according to the manufacturer's instructions.

Cell culture, Slc26a9 knockdown, and ^{36}Cl efflux procedures

Cultured cells from mouse cortical collecting duct (M-1 CCD) and medullary collecting duct (mIMCD-2K) were obtained from American Type Culture Collection (Manassas, VA, USA). mIMCD-2K cells were cultured in Eagle's minimum essential medium supplemented with penicillin (120 IU/ml), streptomycin (120 μg/ml), and 10 % fetal bovine serum. Cells were maintained at 37 °C in a humidified environment of 5 % CO_2 in air. Cells were seeded in 50 mm Petri dishes or 24-well plates and allowed to reach ~90 % confluence before being used for experiments. The Silencer Select Pre-designed SiRNAs for Slc26a9 (ID nos. s233820, s115892, and s115893) and a negative/scrambled control, along with Silencer SiRNA Transfection II Kit (no. AM1631), were purchased from Ambion (Austin, TX, USA). mIMCD-2K cells were transfected by SiRNAa using the transfection kit. Flux experiments were performed 3 days after transfection.

The ^{36}Cl efflux in cultured cells was assayed as before [41]. Briefly, cells were preloaded with ^{36}Cl by preincubation with 2 mM ^{36}Cl added to a solution that contained 100 mM Na-gluconate, 30 mM K-gluconate, and 10 mM HEPES at pH 7.4 for 60 min. Thereafter, the efflux of ^{36}Cl into a low K^+ (2 mE) media with no extracellular chloride (all gluconate salts) was assayed at pH 7.4. The reaction was terminated at either time 0 (no efflux; control) or 10 min (efflux) using cold saline, and the radioactivity of the cells was determined by liquid scintillation spectroscopy [30].

RNA isolation and Northern hybridization

Total cellular RNA was extracted from the kidney cortex according to established methods, quantitated spectrophotometrically, and stored at −80 °C. Hybridization was performed according to established protocols. For pendrin hybridization, a PCR fragment encoding nucleotides 1473–1961 was generated from rat kidney using oligonucleotide primers 5′-CAT TCT GGG GCT GGA CCT C and 5′-CCT TCG GGA CAT TCA CTT TCA C (GenBank accession no. AF-167412). The rat angiotensinogen cDNA probe was a PCR fragment encoding nucleotides 388 to 696 (GenBank accession no. NM_134432). For the amplification of aldosterone synthase in the

adrenal gland, the following primers: 5′-ACCATGGATGTCCAGCAA-3′ (sense) and 5′-GAGAGCTGCCGAGTCTGA-3′ (antisense), corresponding to nucleotides 559 to 856 (GenBank accession no. NM_012538) were used. The DNA fragments used to label apical Na–K–2Cl cotransporter (NKCC2), Na–Cl cotransporter (NCC), and Na channel subunits were the same as before [21, 23, 24].

Western blot analysis

Membrane proteins isolated from mouse kidney cortex were size-fractionated by SDS-PAGE (30 μg/lane) and transferred to nitrocellulose membranes. Membranes were blocked with 5 % milk proteins and then incubated for 6 h with pendrin-specific antibodies. The secondary antibody was a donkey antirabbit IgG-conjugated to horseradish peroxidase (Pierce, Rockford, IL, USA). Pendrin antibodies were generated in our laboratory [11]. The bands were visualized using the chemiluminescence method (RapidStep ECL Reagent, San Diego, CA, USA) and captured on light-sensitive imaging film (MidSci, St. Louis, MO, USA). The dilution for pendrin antibodies was 1/400.

Blood pressure monitoring

Systolic blood pressure in conscious mice was determined using a tail-cuff sphygmomanometer (Visitech BP2000; Visitech Systems, Apex, NC, USA) [40, 41]. Measurements for each mouse represent the mean value of three consecutive recordings performed in the last week of experiments. All experimental animals were preconditioned for blood pressure measurements as before. For long-term salt loading studies, animals were first placed on normal-salt (1 %) liquid diet and after acclimation were switched to high-salt (7 %) liquid diet for 2 weeks. Blood pressures were recorded during the last 3 days of normal-salt diet and the first 2 days and the last 2 days of high-salt diet.

Statistical analysis

The results for chloride excretion, urine volume, urine osmolarity, and blood pressure are presented as the means ± SE. Statistical significance between WT and ESCC knockout mice was determined by Student's paired or unpaired t test, and $p<0.05$ was considered significant.

Results

Distribution and subcellular localization of Slc26a9 in the kidney

Figure 1a shows the mRNA expression of Slc26a9 in the kidney cortex and medulla (top panel) and in cultured cortical (M-1 CCD) and medullary (mIMCD-2K) collecting duct cells (bottom panel). The results indicate a twofold higher expression levels in the medulla and cultured IMCD cells relative to cortex and CCD cells, respectively ($n=3$ in each group). Immunofluorescence labeling of thinly cut kidney sections with Slc26a9-specific antibodies demonstrated apical labeling in a subset of cells in OMCD and the initial IMCD (Fig. 1b (b, c)), with no labeling in the cortex (Fig. 1b (a)). The labeling was completely absent in kidneys of Slc26a9 KO mice (Fig. 1b (d)). To identify the collecting duct cell types expressing Slc26a9, double immunolocalization experiments were performed using

antibodies against Slc26a9 and AQP2. As indicated, Slc26a9 and AQP2 colocalize to the same membrane domain in the medullary collecting duct (Fig. 1c).

Given the specificity of AQP2 labeling, these results demonstrate that Slc26a9 is expressed on the apical membrane of principal cells. For comparison, we examined the localization of Slc26a11 (KBAT) in the kidney [30]. As shown, the expression of Slc26a11 is distinct from Slc26a9 and is exclusively detected in intercalated cells (Fig. 1d).

Effect of Slc26a9 downregulation on $^{36}Cl^-$ efflux in cultured medullary collecting duct cells

To determine the role of Slc26a9 in chloride transport, mIMCD-2K cells were cultured and then transfected with Slc26a9-specific SiRNA (see the “Materials and methods” section). The expression of Slc26a9 decreased by ~65 %, as assessed by semiquantitative reverse transcription polymerase chain reaction (RT-PCR). The efflux of ^{36}Cl in cultured cells, assayed according to the “Materials and methods” section, was reduced by ~31 % in cells that were treated with SiRNA relative to a negative/scrambled SiRNA (n=4 in each group, p<0.05 vs. scrambled SiRNA) (Fig. 2a).

Effects of Slc26a9 deletion on plasma electrolytes and acid–base composition

Blood chemistry data depicted in Table 1 show that blood electrolytes composition in Slc26a9 KO mice is similar to that of WT mice. No acid–base disturbances are noted in Slc26a9 KO mice, as shown by blood pH and plasma HCO_3^- concentration (Table 1). Further, urinary NH_4^+ excretion was not significantly different between Slc26a9 KO and their WT littermates (11.33±2.9 vs. 8.41±0.81 μmol/day, p>0.05, n=5 in each group).

Balanced studies in Slc26a9$^{+/+}$ and Slc26a9$^{-/-}$ *mice*

WT and Slc26a9 KO mice (n=5 in each group) were placed in metabolic cages with free access to rodent chow and distilled water for 3 days. After acclimation, several physiologic parameters were measured daily for two consecutive days. The results, depicted in Table 2, indicate that there was no significant difference in body weight and food or water intake in WT and KO mice.

Given its apical localization in medullary collecting ducts and its function as a chloride transporter/channel [26, 28, 29], we examined the role of Slc26a9 in renal chloride excretion in two models of altered fluid homoeostasis: water deprivation and salt loading.

Response to water deprivation

Slc26a9$^{+/+}$ and Slc26a9$^{-/-}$ mice (n=4 in each group) were placed in metabolic cages and after acclimatization were subjected to 24 h of water deprivation. The body weights and food intake after 24 h of water deprivation are depicted in Table 3 and show no significant difference. Figure 2b, c displays the 24-h urine output and urine osmolality before and after water deprivation. While the urine output decreased and urine osmolality increased in both WT and Slc26a9 KO mice in response to water deprivation, the magnitude of these changes was more pronounced in Slc26a9 KO mice relative to WT littermates. The expression of Slc26a9 in kidneys of WT mice at baseline and after water deprivation was examined. The results demonstrate comparable expression and distribution pattern for Slc26a9 in kidney

medullary collecting duct at baseline state or after water deprivation (data not shown). No Slc26a9 labeling was detected in the cortex after water deprivation (data not shown).

Figure 2d depicts the 24-h urine chloride excretion before and after water deprivation and indicates a significant reduction in urinary chloride excretion in Slc26a9 KO vs. WT mice after 24 h of water deprivation ($p<0.05$). Figure 2e shows sodium excretion before and after water deprivation. It indicates that, while sodium excretion was lower in Slc26a9 KO mice, it did not achieve statistical significance in Slc26a9 KO vs. WT mice after water deprivation (NS=not significant=$p>0.05$).

To determine whether the reduction in urine output and chloride excretion and the increase in urine osmolality in Slc26a9 KO mice vs. WT littermates (Fig. 2) were secondary to a more severe volume depletion, hematocrit levels in WT and Slc26a9 KO mice were measured before and after water deprivation in a separate set of animals. Results were as follows: baseline hematocrit levels were 39.5±0.7 and 38.8±1 % in WT and Slc26a9 KO mice, respectively ($p>0.05$, $n=4$ in each group) and increased to 45.7±1 and 45.5±0.6 % in WT and KO mice, respectively, after 24 h of water deprivation ($p>0.05$, $n=4$ in each group). These results suggest that the more significant reduction in urine output and chloride excretion and the increase in urine osmolality in Slc26a9 KO mice were not due to a more severe dehydration status in the KO mice, but rather reflect the impact of Slc26a9 deletion on these parameters in water deprivation.

Response to salt loading

Next, we examined the urine chloride excretion rates in Slc26a9 KO mice and WT littermates in response to increased dietary salt intake. Animals were placed in regular cages, with free access to a normal-salt (1 %) liquid diet for 1 week. For balanced studies, animals were then placed in metabolic cages while on normal-salt liquid diet and after 48 h were switched to a high-salt (7 %) liquid diet for an additional 4 days. Liquid diet intake, urine volume, and urinary chloride excretion were measured daily.

The results demonstrated that, while liquid diet intake is similar in both groups during the entire duration of experiment (Fig. 3a), urine volume (Fig. 3b), urine chloride (Fig. 3c), and urine sodium (Fig. 3d) excretion rates are significantly reduced in Slc26a9 KO mice during the first 24 h after switching to the high-salt diet, as compared to their WT littermates. These parameters returned to values observed in WT mice after 48 h on high-salt diet (Fig. 3b, c).

Systemic arterial pressure in Slc26a9 KO and their WT littermates at baseline and in response to salt loading

Next, we sought to examine the systemic arterial pressure in Slc26a9 KO animals at baseline state (see the “Materials and methods” section). Figure 4a shows the average of blood pressure measurements for three consecutive days in conscious Slc26a9 WT and KO mice with a computerized tail-cuff sphygmomanometer (Visitech BP2000; Visitech Systems, Apex, NC, USA). The results demonstrate that Slc26a9 KO mice have significantly elevated arterial pressure (142±7 mmHg in Slc26a9 KO mice and 117±7 mmHg in WT mice, $p<0.02$, $n=4$ in each group; Fig. 4a).

While it is likely that several factors might be at work to increase the blood pressure in Slc26a9 KO mice, given the role of Slc26a9 in chloride excretion (Figs. 2 and 3), we examined the impact of high-salt diet on blood pressure in Slc26a9 KO mice. Slc26a9 KO animals were placed on normal-salt (1 %) liquid diet for 3 days and then switched to a high-salt (7 %) liquid diet. Figure 4b demonstrates that Slc26a9 KO mice significantly increased their blood pressure within the first 48 h of switching to the high-salt diet, with values increasing from 134±5.6 to 153±2.5 mmHg at 48 h ($p<0.005$ after 48 h on high-salt diet). The increase in blood pressure at 24 h after salt loading barely missed the statistical significance mark ($p>0.05$ but <0.06). WT ($Slc26a9^{+/+}$) mice on high-salt diet for the same duration did not display any significant elevation in their systolic blood pressure, with values of 109±4.1 mmHg at baseline state and 113±4.4 and 112±4.7 mmHg at 24 and 48 h after switching to the high-salt diet ($p>0.05$ vs. baseline for both 24 and 48 h time points, $n=4$). Interestingly, blood pressure measurements in Slc26a9 KO and WT mice, performed after 2 weeks on high-salt diet (Fig. 4c), showed values very similar to those observed in animals on normal salt intake (Fig. 4a).

Our next series of studies focused on the expression of chloride- and/or sodium-absorbing transporters in the kidney tubules. Toward this end, we examined the expression of pendrin, the major chloride-reabsorbing transporter in the distal nephron. As shown, pendrin mRNA levels and protein abundance increased significantly in kidneys of Slc26a9 KO mice on normal-salt diet ($n=3$ in each group; Fig. 5a, b). We have examined the expression of H^+-ATPase in kidneys of Slc26a9 KO mice, using a monoclonal antibody against the 31-kDa subunit. The results show comparable expression and distribution patterns for H^+-ATPase in kidneys of both genotypes (data not shown).

The mRNA expression levels of apical NKCC2 (also known as BSC1) and the thiazide-sensitive NCC, two major sodium- and chloride-absorbing transporters in the distal nephron, remained unchanged in Slc26a9 KO mice (Fig. 6a). Immunofluorescence labeling studies indicated comparable apical distribution and intensity levels of NKCC2 in the thick limb of Henle of Slc26a9 KO and WT mice (data not shown). The kidney expression of Na channel subunits remained unchanged in Slc26a9 KO mice (Fig. 6b). Additional studies demonstrated that the expression of angiotensinogen increased in kidneys of KO mice under basal conditions (Fig. 6c). The expression of aldosterone synthase in the adrenal gland, a sensitive step in aldosterone synthesis, remained unchanged in KO animals relative to WT littermates (Fig. 6d).

Discussion

Functional studies have demonstrated the presence of secretory chloride channels in apical membranes of cultured medullary collecting duct cells; however, little is known about the molecular identity of such channels/pathways [12–14]. Both the ADH/cAMP-sensitive and the calcium-stimulated chloride channels have been identified in mIMCD-K2 cells, which are derived from mouse medullary collecting ducts [13, 31, 32]. However, the role of these channels in salt homeostasis in vivo has not been examined. While the cystic fibrosis transmembrane regulator (CFTR) may play a role in cAMP-sensitive electrogenic chloride secretion in cultured IMCD cells [13, 14, 31], there are no studies demonstrating any

renal electrolyte excretion impairments in mouse models of cystic fibrosis. Taken together, published reports support the presence of molecules other than CFTR as major players in electrogenic chloride secretion in IMCD.

The most salient features of the current studies are the identification of Slc26a9 as a regulator of renal salt (chloride and sodium) excretion and systemic arterial pressure, specifically during salt loading. These conclusions are based on the following findings: (1) Localization of Slc26a9 to the apical membrane of principal cells in the medullary collecting duct (Fig. 1), (2) decreased chloride and sodium excretion in Slc26a9 KO mice upon switching to a high-salt diet (Fig. 3), and (3) elevated systemic arterial pressure in Slc26a9 null mice (Fig. 4). Taken together, these results suggest that Slc26a9 mediates chloride excretion and regulates systemic arterial pressure.

Slc26a9 can function as a chloride channel as well as a Cl^-/HCO_3^- exchanger in in vitro expression systems [26, 28, 29]. Given the low urine pH and near-zero concentration of bicarbonate in the lumen of medullary collecting duct under baseline conditions, we suggest that Slc26a9 predominantly functions as a chloride channel in IMCD cells.

Slc26a9 KO mice display systemic hypertension. This phenotype provides new insight into the role of Slc26a9 in systemic blood pressure control. Given the role of Slc26a9 in chloride excretion (see the “Results” section), it is plausible that the systemic hypertension in Slc26a9 KO mice is in part due to the impaired salt excretion. Slc26a9 KO mice increase their arterial pressure significantly within 48 h of switching to a high-salt diet (Fig. 4b), which correlated with the impaired salt excretion during the same period (Fig. 4). If Slc26a9 KO mice demonstrate significant reduction in salt (chloride and sodium) excretion only when fed a diet high in salt, why are they hypertensive under baseline conditions? In response, we should point to the possibility that there might be more than one reason for elevated blood pressure in Slc26a9 KO mice, including possible enhanced chloride absorption via pendrin or increased vascular resistance. Given the role of Slc26a9 in chloride excretion, one possibility, however, could be the gradual retention of salt over a long period, with the subsequent activation of compensatory mechanisms that can normalize salt excretion but increase the vascular resistance. Such a possibility has been postulated in several models of salt retention, including in animals or human with primary increase in aldosterone levels. Interestingly, the Slc26a9 KO mice normalized their salt excretion after 48 h (Fig. 3) and, surprisingly, the initial additional elevation in arterial blood pressure in KO mice on high-salt diet disappeared after 2 weeks on high-salt diet (Fig. 4c). It is plausible that mutant mice develop adaptive compensatory mechanisms to excrete the excess salt and prevent further increases in their blood pressure. In support of this latter possibility, we observe a significant reduction in pendrin abundance in kidneys of Slc26a9 KO mice on a high-salt diet (data not shown). The sodium retention during the early phase of salt loading in Slc26a9 KO mice (Fig. 3) is likely caused by enhanced sodium reabsorption via ENaC in the collecting duct secondary to altered transmembrane potential subsequent to reduced chloride secretion via Slc26a9. Whether systemic factors can contribute to the elevated blood pressure in Slc26a9 KO mice remain speculative. Possibilities such as Slc26a9 playing a role in aldosterone synthesis by the adrenal gland or controlling the vascular resistance by regulating salt uptake in vascular smooth muscle cells need to be considered. Expression

studies by RT-PCR did not demonstrate any Slc26a9 mRNA in the vascular smooth muscle cells or the adrenal gland. The expression of angiotensinogen was found to be increased in the kidneys of Slc26a9 KO mice (Fig. 6c); however, the expression of aldosterone synthase, a very sensitive enzyme in the aldosterone synthesis pathway, remained unchanged in KO mice vs. WT littermates (Fig. 6d).

It is well known that water deprivation, which increases serum osmolarity [33–35], leads to a disproportionate increase in salt excretion relative to urine volume, a process known as dehydration natriuresis, which helps prevent a rise in serum chloride and sodium [33]. Recent studies demonstrated that the expression of serum- and glucocorticoid-inducible kinase (Sgk1) in the medullary collecting duct is enhanced by extracellular tonicity [33] via a tonicity-responsive enhancer (TonE) upstream of the Sgk1 transcriptional start site [33]. This process is under the control of the transcription factor NFAT5 and results in increased expression of the type A natriuretic peptide receptor (NPR-A), causing dehydration natriuresis [33]. We speculate that Slc26a9 is the final effector molecule in the hypertonicity–Sgk1–NFAT–natriuretic peptide pathway in water deprivation and mediates chloride secretion, which can secondarily impair sodium reabsorption via membrane potential alteration, therefore leading to dehydration natriuresis. Our results indicate that, while chloride excretion is decreased significantly in Slc26a9 KO mice relative to WT littermates, urine sodium excretion did not display a proportional reduction in water deprivation, highlighting the specific role of Slc26a9 in chloride excretion (Fig. 2). It is worth mentioning that both urine chloride and sodium excretions rates decreased significantly in salt loading (Fig. 3).

It has been proposed that IMCD cells absorb and secrete fluid and electrolytes, in part via CFTR, and may have a significant role in modulating the composition and volume of the final urine [14, 36–38]. Recent studies demonstrate that Slc26a9 functionally and physically interacts with CFTR and the coexpression of both channels enhances the cAMP-stimulated chloride channel activity [39]. It is, therefore, plausible to consider the (PKA-dependent) cAMP-stimulated chloride channel in IMCD as an interaction of two distinct channels, namely, Slc26a9 and CFTR. In this context, deletion of either Slc26a9 or CFTR leaves the other channel intact but reduces the total chloride channel activity. This hypothesis can be tested in mutant animals with double knockout for CFTR and Slc26a9.

In conclusion, Slc26a9 is expressed on the apical membrane of principal cells in the medullary collecting ducts and plays an important role in renal salt/fluid excretion and blood pressure regulation. We propose that impaired SLC26A9 activity, either due to single nucleotide polymorphism or in response to epigenetic factors can play a role in the pathogenesis of hypertension in humans.

Acknowledgments

These studies were supported by a Merit Review Grant from the Department of Veterans Affairs, a grant from NIH (R56 DK 62809), and by grants from US Renal Care (to M.S.).

References

1. Schwartz GJ, Barasch J, Al-Awqati Q (1985) Plasticity of functional epithelial polarity. Nature 318(6044):368–371 [PubMed: 2415824]
2. Schuster VL (1993) Function and regulation of collecting duct intercalated cells. Annu Rev Physiol 55:267–288 [PubMed: 8466177]
3. Silver RB, Soleimani M (1999) H^+-K^+-ATPases: regulation and role in pathophysiological states. Am J Physiol Renal Physiol 276:F799–F811
4. Gamba G (2005) Role of WNK kinases in regulating tubular salt and potassium transport and in the development of hypertension. Am J Physiol Renal Physiol 288(2):F245–F252 [PubMed: 15637347]
5. Ishibashi K, Hara S, Kondo S (2009) Aquaporin water channels in mammals. Clin Exp Nephrol 13(2):107—117 [PubMed: 19085041]
6. Soundararajan R, Pearce D, Hughey RP, Kleyman TR (2010) Role of epithelial sodium channels and their regulators in hypertension. J Biol Chem 285(40):30363–30369 [PubMed: 20624922]
7. Greenlee MM, Lynch IJ, Gumz ML, Cain BD, Wingo CS (2010) The renal H,K-ATPases. Curr Opin Nephrol Hypertens 19(5):478–482 [PubMed: 20616716]
8. Soleimani M, Greeley T, Petrovic S, Wang Z, Amlal H, Kopp P, Burnham CE (2010) Pendrin: an apical $Cl^-/OH^-/HCO_3^-$ exchanger in the kidney cortex. Am J Physiol Renal Physiol 280:F356–F364
9. Royaux IE, Wall SM, Karniski LP, Everett LA, Suzuki K, Knepper MA, Green ED (2001) Pendrin, encoded by the Pendred syndrome gene, resides in the apical region of renal intercalated cells and mediates bicarbonate secretion. Proc Natl Acad Sci U S A 98:4221–4226 [PubMed: 11274445]
10. Verlander JW, Hassell KA, Royaux IE, Glapion DM, Wang ME, Everett LA, Green ED, Wall SM (2003) Deoxycorticosterone upregulates PDS (Slc26a4) in mouse kidney: role of pendrin in mineralocorticoid-induced hypertension. Hypertension 179:356–362
11. Amlal H, Petrovic S, Xu J, Wang Z, Sun X, Barone S, Soleimani M (2010) Deletion of the anion exchanger Slc26a4 (pendrin) decreases apical Cl(−)/HCO3(−) exchanger activity and impairs bicarbonate secretion in kidney collecting duct. Am J Physiol Cell Physiol 299(1):C33–C41 [PubMed: 20375274]
12. Boese SH, Aziz O, Simmons NL, Gray MA (2004) Kinetics and regulation of a Ca^{2+}-activated Cl^- conductance in mouse renal inner medullary collecting duct cells. Am J Physiol Renal Physiol 286:F682–F692 [PubMed: 14678946]
13. Boese SH, Glanville M, Aziz O, Gray MA, Simmons NL (2000) Ca^{2+} and cAMP-activated Cl^- conductances mediate Cl^- secretion in a mouse renal inner medullary collecting duct cell line. J Physiol 523(Pt 2):325–338 [PubMed: 10699078]
14. Wallace DP, Christensen M, Reif G, Belibi F, Thrasher B, Herrell D, Grantham JJ (2002) Electrolyte and fluid secretion by cultured human inner medullary collecting duct cells. Am J Physiol Renal Physiol 283(6):F1337–F1350 [PubMed: 12388381]
15. Lohi H, Kujala M, Kerkela E, Saarialho-Kere U, Kestila M, Kere J (2000) Mapping of five new putative anion transporter genes in human and characterization of SLC26A6, a candidate gene for pancreatic anion exchanger. Genomics 70:102–112 [PubMed: 11087667]
16. Lohi H, Kujala M, Makela S, Lehtonen E, Kestila M, Saarialho-Kere U, Markovich D, Kere J (2002) Functional characterization of three novel tissue-specific anion exchangers SLC26A7, -A8, and -A9. J Biol Chem 277:14246–14254 [PubMed: 11834742]
17. Romero MF, Chang MH, Plata C, Zandi-Nejad K, Mercado A, Broumand V, Sussman CR, Mount DB (2006) Physiology of electrogenic SLC26 paralogues. Novartis Found Symp 273:126–138 [PubMed: 17120765]
18. Soleimani M (2006) Expression, regulation and the role of SLC26 Cl^-/HCO_3^- exchangers in kidney and gastrointestinal tract. Novartis Found Symp 273:91–102 [PubMed: 17120763]
19. Soleimani M, Xu J (2006) SLC26 chloride/base exchangers in the kidney in health and disease. Semin Nephrol 26:375–385 [PubMed: 17071331]
20. Alper SL, Stewart AK, Chernova MN, Zolotarev AS, Clark JS, Vandorpe DH (2006) Anion exchangers in flux: functional differences between human and mouse SLC26A6 polypeptides. Novartis Found Symp 273:107–119 [PubMed: 17120764]

21. Schweinfest CW, Spyropoulos DD, Henderson KW, Kim JH, Chapman JM, Barone S, Worrell RT, Wang Z, Soleimani M (2006) Slc26a3 (dra)-deficient mice display chloride-losing diarrhea, enhanced colonic proliferation, and distinct upregulation of ion transporters in the colon. J Biol Chem 281:37962–37971 [PubMed: 17001077]
22. Wang Z, Petrovic S, Mann E, Soleimani M (2002) Identification of an apical Cl^-/HCO_3^- exchanger in the small intestine. Am J Physiol 282:G573–G579
23. Wang Z, Wang T, Petrovic S, Tuo B, Riederer B, Barone S, Lorenz JN, Seidler U, Aronson PS, Soleimani M (2005) Renal and intestine transport defects in Slc26a6-null mice. Am J Physiol Cell Physiol 288:C957–C965 [PubMed: 15574486]
24. Xu J, Song P, Nakamura S, Miller M, Barone S, Alper SL, Riederer B, Bonhagen J, Arend LJ, Amlal H et al. (2009) Deletion of the chloride transporter slc26a7 causes distal renal tubular acidosis and impairs gastric acid secretion. J Biol Chem 284(43):29470–29479 [PubMed: 19723628]
25. Xu J, Henriksnas J, Barone S, Witte D, Shull GE, Forte JG, Holm L, Soleimani M (2005) SLC26A9 is expressed in gastric surface epithelial cells, mediates Cl^-/HCO_{3-} exchange, and is inhibited by NH^{4+}. Am J Physiol Cell Physiol 289:C493–C505 [PubMed: 15800055]
26. Xu J, Song P, Miller ML, Borgese F, Barone S, Riederer B, Wang Z, Alper SL, Forte JG, Shull GE et al. (2008) Deletion of the chloride transporter Slc26a9 causes loss of tubulovesicles in parietal cells and impairs acid secretion in the stomach. Proc Natl Acad Sci U S A 105(46):17955–17960 [PubMed: 19004773]
27. Kim KH, Shcheynikov N, Wang Y, Muallem S (2005) SLC26A7 is a Cl^- channel regulated by intracellular pH. J Biol Chem 280:6463–6470 [PubMed: 15591059]
28. Dorwart MR, Shcheynikov N, Wang Y, Stippec S, Muallem S (2007) SLC26A9 is a Cl^- channel regulated by the WNK kinases. J Physiol 584:333–345 [PubMed: 17673510]
29. Chang MH, Plata C, Zandi-Nejad K, Sindić A, Sussman CR, Mercado A, Broumand V, Raghuram V, Mount DB, Romero MF (2009) Slc26a9—anion exchanger, channel and Na^+ transporter. J Membr Biol 228(3):125–140 [PubMed: 19365592]
30. Xu J, Barone S, Li H, Holiday S, Zahedi K, Soleimani M (2011) Slc26a11, a chloride transporter, localizes with the vacuolar H(+)-ATPase of A-intercalated cells of the kidney. Kidney Int 80(9):926–937 [PubMed: 21716257]
31. Van Huyen JP, Bens M, Teulon J, Vandewalle A (2001) Vasopressin-stimulated chloride transport in transimmortalized mouse cell lines derived from the distal convoluted tubule and cortical and inner medullary collecting ducts. Nephrol Dial Transplant 16(2):238–245 [PubMed: 11158395]
32. Kose H, Boese SH, Glanville M, Gray MA, Brown CD, Simmons NL (2000) Bradykinin regulation of salt transport across mouse inner medullary collecting duct epithelium involves activation of a Ca(2+)-dependent Cl(−) conductance. Br J Pharmacol 131(8):1689–1699 [PubMed: 11139448]
33. Chen S, Grigsby CL, Law CS, Ni X, Nekrep N, Olsen K, Humphreys MH, Gardner DG (2009) Tonicity-dependent induction of Sgk1 expression has a potential role in dehydration-induced natriuresis in rodents. J Clin Invest 119(6):1647–1658 [PubMed: 19436108]
34. Bartolo RC, Donald JA (2008) The effect of water deprivation on the tonicity responsive enhancer binding protein (TonEBP) and TonEBP-regulated genes in the kidney of the Spinifex hopping mouse, *Notomys alexis*. J Exp Biol 211(Pt 6):852–859 [PubMed: 18310110]
35. Stein CS, Yancey PH, Martins I, Sigmund RD, Stokes JB, Davidson BL (2010) Osmoregulation of ceroid neuronal lipofuscinosis type 3 in the renal medulla. Am J Physiol Cell Physiol 298(6):C1388–C1400 [PubMed: 20219947]
36. Rajagopal M, Pao AC (2010) Adenosine activates a2b receptors and enhances chloride secretion in kidney inner medullary collecting duct cells. Hypertension 55(5):1123–1128 [PubMed: 20308611]
37. Wallace DP, Rome LA, Sullivan LP, Grantham JJ (2001) cAMP-dependent fluid secretion in rat inner medullary collecting ducts. Am J Physiol Renal Physiol 280(6):F1019–F1029 [PubMed: 11352842]
38. Kizer NL, Vandorpe D, Lewis B, Bunting B, Russell J, Stanton BA (1995) Vasopressin and cAMP stimulate electrogenic chloride secretion in an IMCD cell line. Am J Physiol 268(5 Pt 2):F854–F861 [PubMed: 7771514]

39. Bertrand CA, Zhang R, Pilewski JM, Frizzell RA (2009) SLC26A9 is a constitutively active, CFTR-regulated anion conductance in human bronchial epithelia. J Gen Physiol 133(4):421–438 [PubMed: 19289574]

40. Singh AK, Amlal H, Haas PJ, Dringenberg U, Fussell S, Barone SL, Engelhardt R, Zuo J, Seidler U, Soleimani M (2008) Fructose-induced hypertension: essential role of chloride and fructose absorbing transporters PAT1 and Glut5. Kidney Int 74:438–447 [PubMed: 18496516]

41. Barone S, Fussell SL, Singh AK, Lucas F, Xu J, Kim C, Wu X, Yu Y, Amlal H, Seidler U et al. (2009) Slc2a5 (Glut5) is essential for the absorption of fructose in the intestine and generation of fructose-induced hypertension. J Biol Chem 284:5056–5066 [PubMed: 19091748]

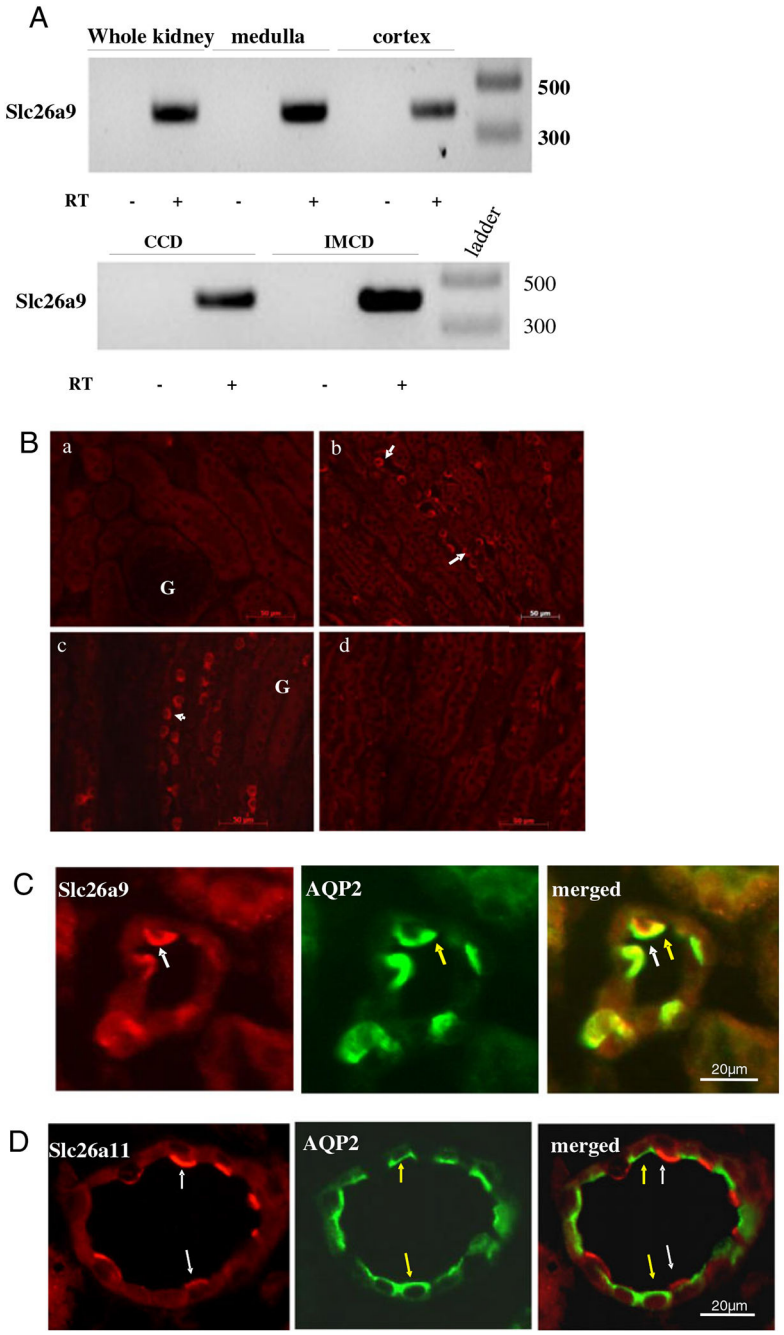

Fig. 1.

Expression and localization of Slc26a9 in the kidney. **a** *Top panel* Slc26a9 expression in the kidney cortex and medulla. RT-PCR experiments demonstrating Slc26a9 transcript in kidney cortex and medulla. *Bottom panel* Slc26a9 expression in cultured collecting duct cells. RT-PCR experiments demonstrating the expression of Slc26a9 in cultured cortical (M-1 CCD) and medullary (mIMCD-2K) collecting duct cells. **b** Immunolocalization of Slc26a9 in the kidney. Slc26a9 antibody labels the apical membrane in a subset of cells in medullary collecting duct (*b*, *c*) but not the cortex (*a*). Labeling with Slc26a9 antibodies

did not detect any signal in the kidneys of Slc26a9 KO mice (*d*). *G* glomerulus. **c** Double immunofluorescent staining with Slc26a9 and AQP2. Merged images of Slc26a9 and AQP2 labeling (*middle panel*) demonstrate the colocalization of Slc26a9 with AQP2 in medullary collecting duct cells. **d** Double immunofluorescent staining with Slc26a11 and AQP2. Merged images of Slc26a11 (KBAT) and AQP2 labeling do not show any colocalization of KBAT with AQP2 in medullary collecting duct cells

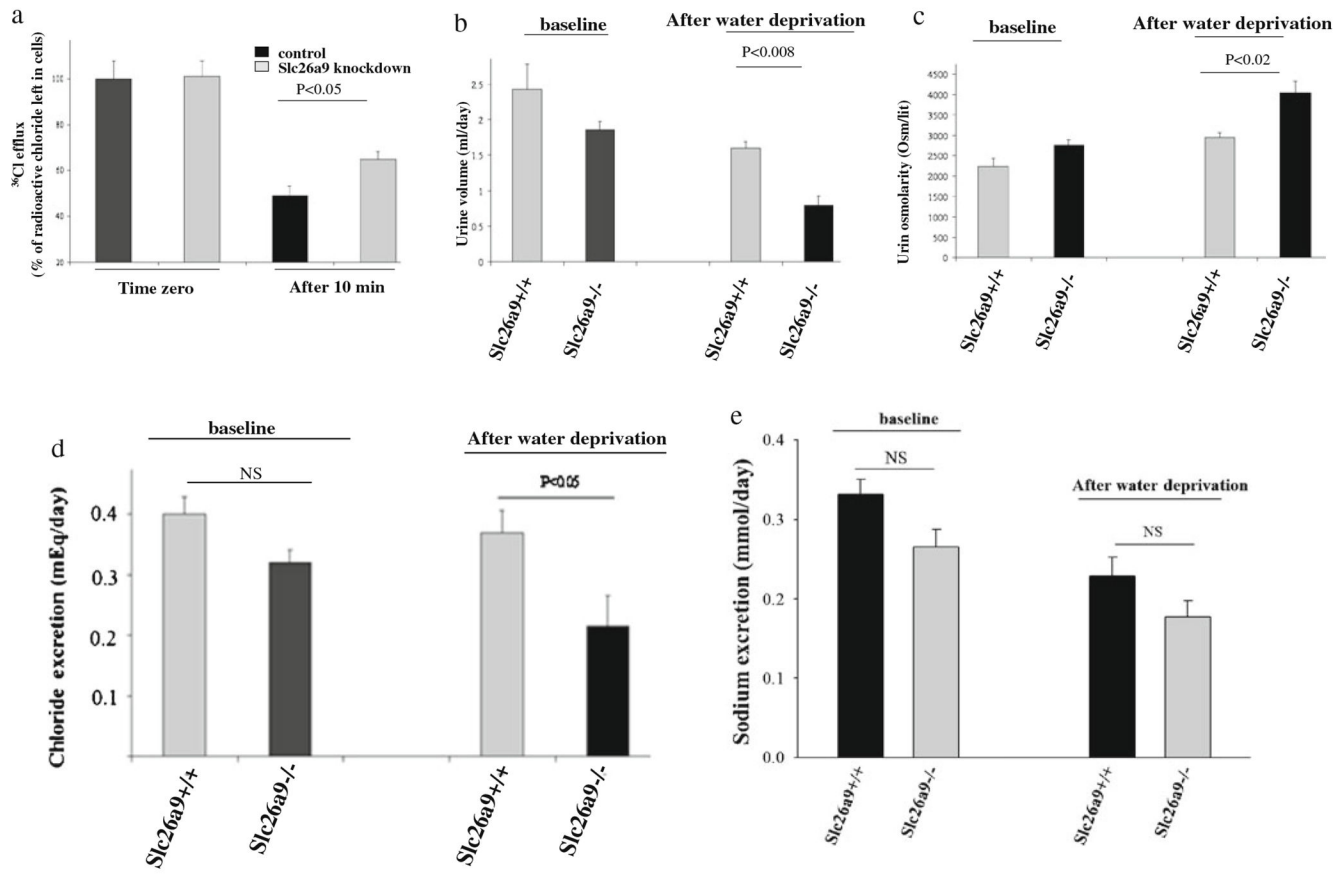

Fig. 2.

Role of Slc26a9 in chloride excretion. **a** Slc26a9 downregulation decreases $^{36}Cl^{-}$ efflux in cultured mIMCD cells. ^{36}Cl efflux was decreased in cultured IMCD cells treated with Slc26a9 SiRNA (for details, see the “Materials and methods” section). **b**, **c** Urine output and osmolality before and after water deprivation in Slc26a9$^{+/+}$ and Slc26a9$^{-/-}$ mice. Urine volume (**b**) significantly decreased whereas urine osmolality (**c**) significantly increased in Slc26a9 KO mice in response to water deprivation. **d** Urine chloride excretion before and after water deprivation. Urine chloride excretion was significantly decreased in Slc26a9 KO mice after water deprivation. **e** Urine sodium excretion before and after water deprivation. Urine sodium excretion was not significantly affected in Slc26a9 KO mice after water deprivation

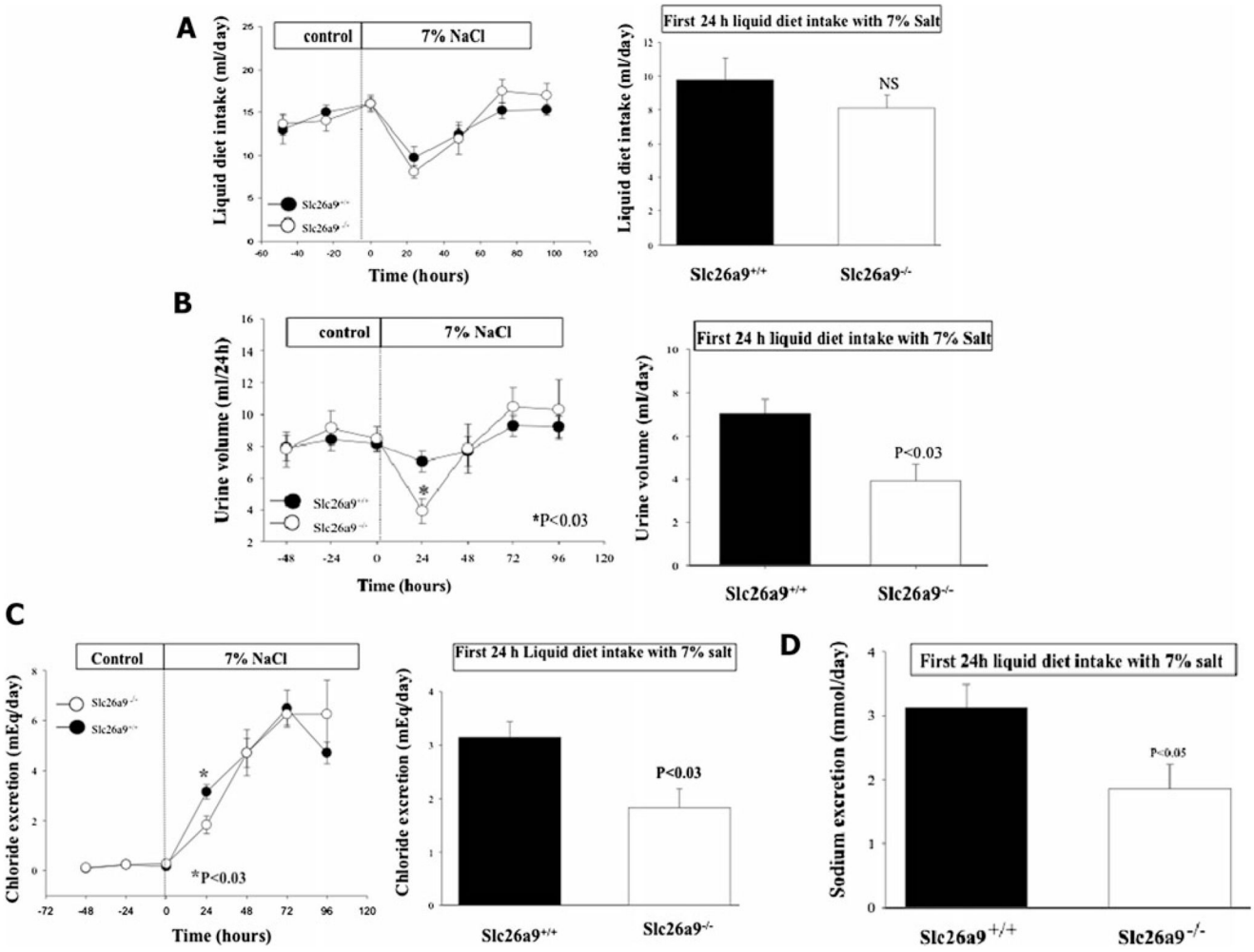

Fig. 3.

The role of Slc26a9 in water intake and fluid and chloride excretion in response to salt loading. **a**, **b** Fluid intake and urine volume in salt loading. The water intake (**a**) was not significantly different, but urine volume (**b**) was significantly decreased in Slc26a9 KO mice in the first 24 h after switching to high-salt diet. The urine output in KO mice returned to values observed in WT animals at 2 days after switching to high-salt diet. **c** Chloride excretion in salt loading. Urine chloride excretion rates were comparable in both genotypes on normal-salt diet but decreased significantly in Slc26a9 KO mice in the first 24 h after switching to a high-salt liquid diet. The chloride excretion rate in KO mice returned to normal levels observed in WT animals. **d** Sodium excretion in salt loading. Similar to **c**, excretion rates for sodium were comparable in both genotypes on normal-salt diet but decreased significantly in Slc26a9 KO mice in the first 24 h of a high-salt diet

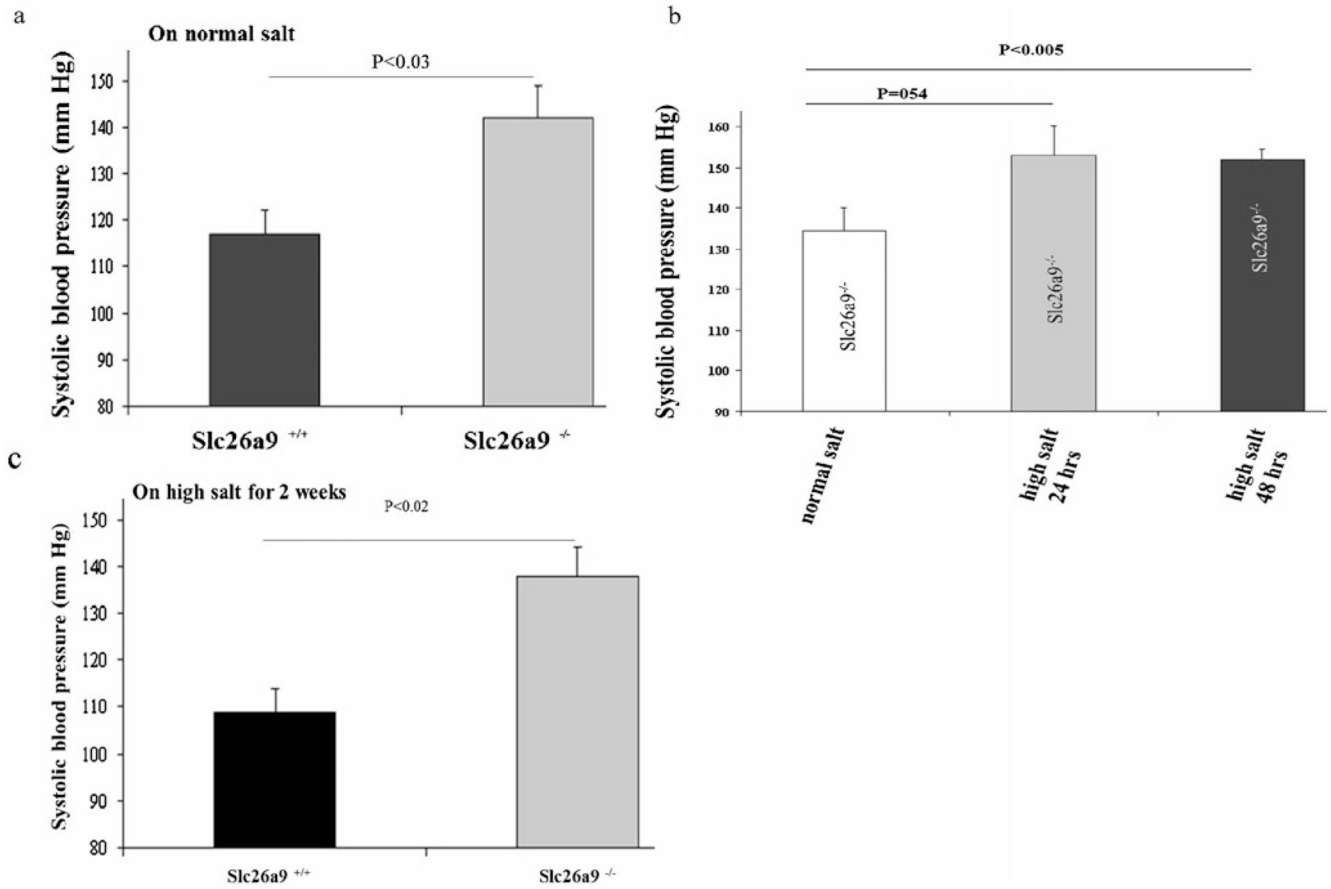

Fig. 4.

Slc26a9$^{-/-}$ mice have systemic hypertension. **a** On normal-salt diet. Systemic blood pressure was measured in conscious mice according to the “Materials and methods” section. Slc26a9 KO mice displayed significant systolic hypertension vs. WT littermates. **b** On high-salt diet for 2 days. Slc26a9 KO mice were placed on a normal-salt (1 %) diet for 3 days and then switched to a high-salt (7 %) diet. Results demonstrate that KO mice increased their blood pressure at 24 and 48 h after switching to the high-salt diet. **c** On high-salt diet for 2 weeks. WT and mutant mice were maintained on a high-salt diet for 2 weeks according to the “Materials and methods” section. Slc26a9 KO mice remained hypertensive on high-salt diet with no significant change on the magnitude of systemic blood pressure relative to the normal-salt diet

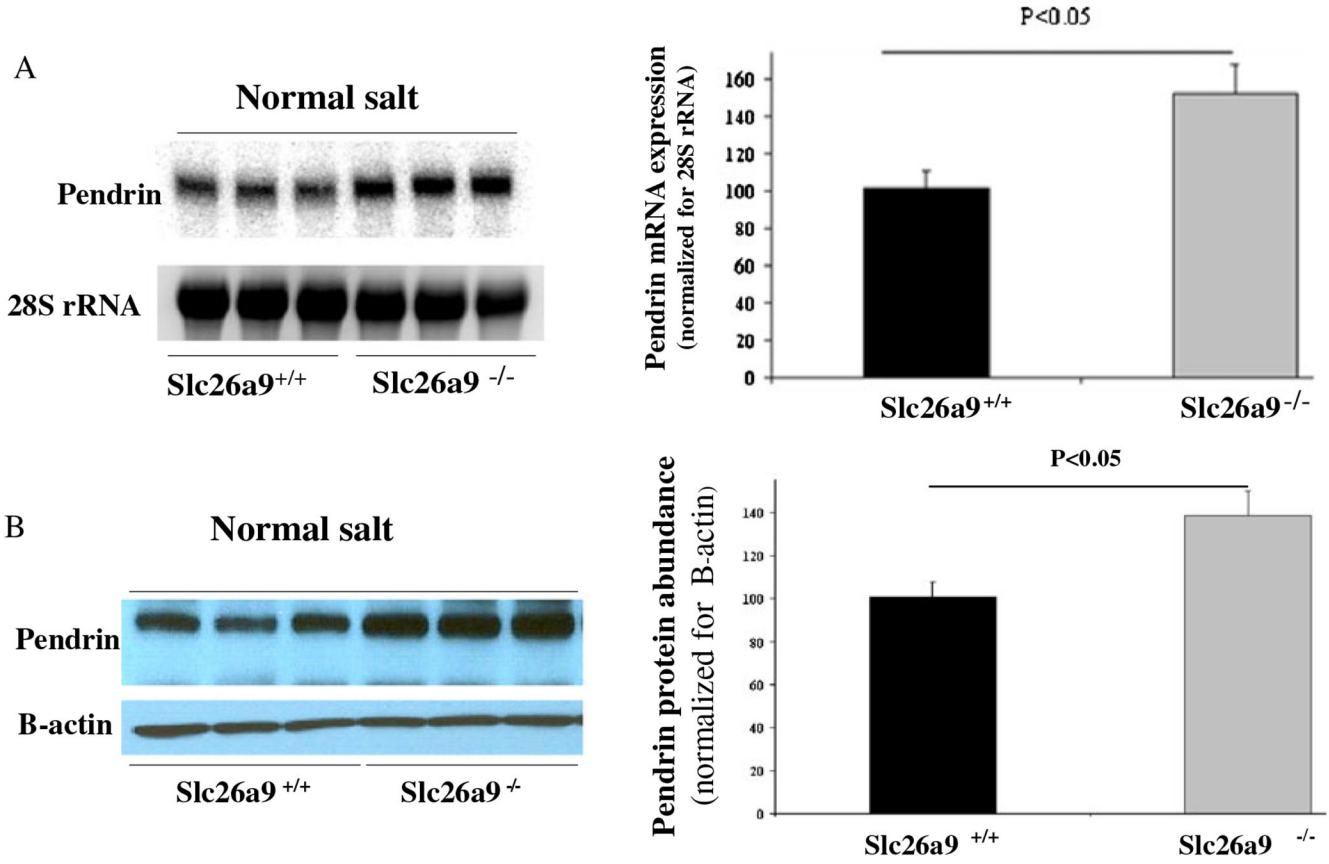

Fig. 5.

Expression of pendrin in the kidneys of Slc26a9 KO mice under basal conditions. **a**, **b** Regulation of pendrin in kidneys of Slc26a9$^{-/-}$ mice. **a** Northern hybridization; **b** Western blotting. Results show the upregulation of pendrin in kidneys of Slc26a9$^{-/-}$ mice under baseline conditions

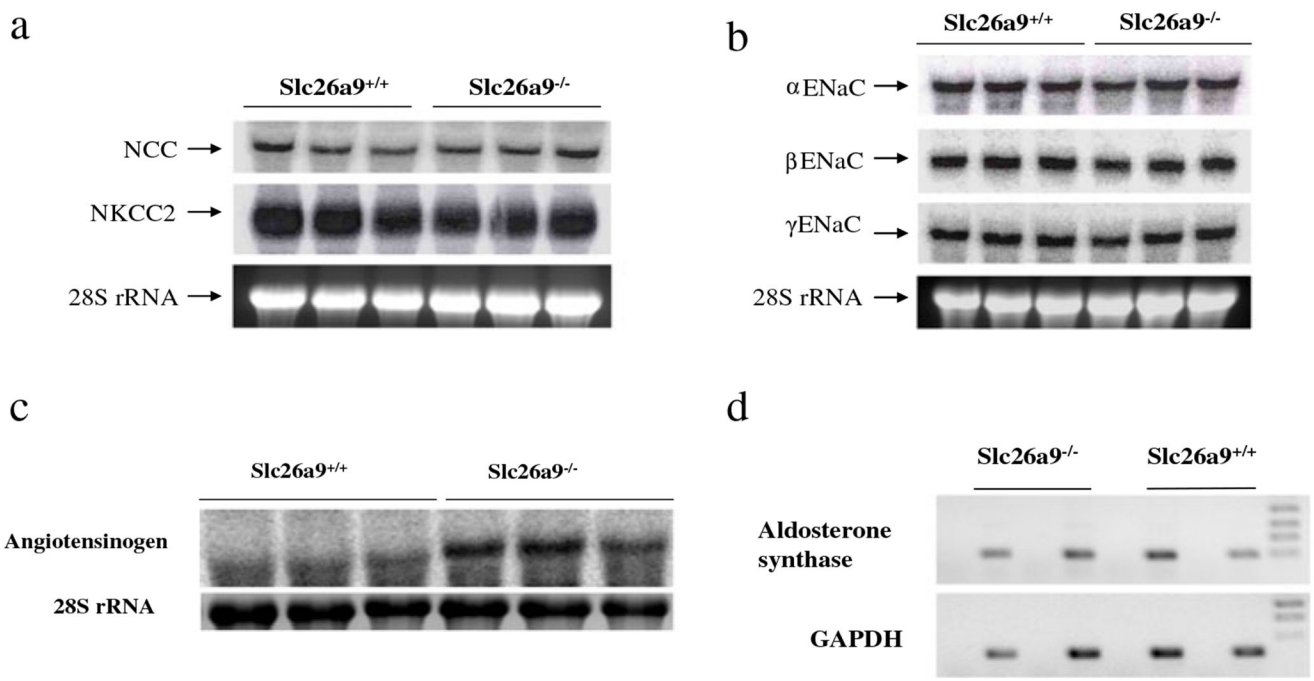

Fig. 6.

Expression of distal nephron ion transporters and agiotensinogen in kidneys of Slc26a9$^{+/+}$ and Slc26a9$^{-/-}$. **a** NKCC2 and NCC expression. Expression of NCC and NKCC2 remained unchanged in kdineys of Slc26a9$^{-/-}$ mice. **b** Sodium channel subunits expression by northern hybridization. mRNA expression of ENaC subunits remained unchanged in kidneys of Slc26a9$^{-/-}$ mice. **c** Expression of angiotensinogen increased in kidneys of Slc26a9−/− mice. mRNA expression of angiotensinogen increased in kidneys of Slc26a9−/− mice. **d** Expression of aldosterone synthase in adrenal glands of Slc26a9$^{+/+}$ and Slc26a9$^{-/-}$ mice. Semi-quantitative RT-PCR shows that the expression of aldosterone synthase remained unchanged in adrenal glands of Slc26a9$^{-/-}$ mice (n=4 for each group)

Table 1

Blood composition in Slc26a9$^{+/+}$ and Slc26a9$^{-/-}$ mice at steady state

	pH (pH units)	PCO_2 (mmHg)	[HCO_3^-] (mmol/L)	[Na^+] (mmol/L)	[K^+] (mmol/L)	[Cl^-] (mmol/L)	[iCa^{++}] (mg/day)
Slc26a9$^{+/+}$	7.37±0.02	45±2.33	26±1.19	140±1.49	4.70±0.24	101±0.28	1.04±0.07
p value	NS	NS	NS	NS	NS	NS	NS
Slc26a9$^{-/-}$	7.36±0.004	48±1.73	27±1.12	138±1.76	4.90±0.17	102±0.39	0.95±0.03

Data are presented as the mean±SEM. *N*=5 mice in each group

NS not significant

Table 2

Physiologic data in Slc26a9$^{+/+}$ and Slc26a9$^{-/-}$ mice at steady state

	Slc26a9$^{+/+}$	***p* value**	**Slc26a9$^{-/-}$**
Body weight (g)	26±0.27	NS	27±1.04
Food intake (g/day)	3.90±0.35	NS	4.30±0.35
Water intake (g/day)	5.70±0.96	NS	4.36±0.22

Data are presented as the mean±SEM. *N*=5 mice in each group

NS not significant

Table 3

Physiologic data in Slc26a9$^{+/+}$ and Slc26a9$^{-/-}$ mice in response to 24 h of water deprivation

	Slc26a9$^{+/+}$	***p* value**	**Slc26a9$^{-/-}$**
Body weight (g)	23±0.27	NS	25±1.99
Food intake (g/day)	2.84±0.12	NS	2.40±0.43
Water intake (g/day)	0±0	–	0±0